Response to reviewer #2

We gratefully thank the editor and all reviewers for their time spent making their constructive remarks and useful suggestions, which has significantly raised the quality of the manuscript and has enabled us to improve the manuscript. Each suggested revision and comment, brought forward by the reviewers, was accurately incorporated and considered. Below the comments of the reviewers are responses point by point and the revisions are indicated.

RC2

The manuscript seeks to quantify the relationship between the propagation speed and wavelength of mode-2 ISWs and a number of parameters (e.g. depth). Data is from measurements taken during a field campaign off the coast of Central America. The manuscript is difficult to read and its scientific conclusions are weak. I have worked on mode-2 waves for some time, and the question of propagation speed/wavelength variability never struck me as a pressing issue. This doesn't mean I wouldn't want to read about it, but it does mean I would like some motivation for doing so. The authors hint at links with actual dynamics of the mode-2 waves (lines 30-50) but never really return to these ideas when discussing their results.

Response: Thank you for your comment. Because generally, the seismic oceanography method can only get the "snapshot" of ocean vertical temperature gradient for a long horizontal distance section. It is a little difficult to study the actual dynamics of the mode-2 ISWs during a long period using the seismic oceanography method. The kinematics characteristics of the ISWs we want to describe in lines 30-50 are mainly the characteristics related to the wave propagation speed. We have added the supplementary explanation in the corresponding places in the introduction of the revised manuscript (line 33). We also show the revised text as follow:
Scholars have used the seismic oceanography method to carry out related studies on the geometry and kinematics characteristics (mainly related to propagation speed) of ISW in the South China Sea, the Mediterranean Sea, and the Pacific Coast of Central America (Bai et al., 2017; Fan et al., 2021a, 2021b; Geng et al., 2019; Sun et al., 2019; Tang et al., 2014, 2018).

The authors appear to have some rather basic points of theoretical misunderstanding; for example there is repeated mention of phase velocity, but ISWs do not have a phase velocity. Only linear waves have a well-defined distinction between phase and group speeds, something that goes back (at least) to the classical work of Whitham in the 1960s. In a similar vein, ISWs are "long waves" so why does the frequency appear in the TG equation on line 400?

Response: Thank you for your valuable comment. We feel sorry for our theoretical misunderstanding. We have changed all the "phase velocity" into "propagation speed" in the revised manuscript. We used the frequency $w=0$ in our study when computing the linear vertical mode function by solving TG equation. It is our mistake to add the frequency in the TG equation. We have deleted the frequency in the TG equation in the corresponding place in the revised manuscript (line 463). We also show the revised text as follow:
The linear vertical mode function can be obtained by solving the eigenvalue equation that

satisfies the Taylor-Goldstein problem (Holloway et al., 1999):

$$\frac{d^2\varphi(z)}{dz^2} + \frac{N^2(z)}{C^2}\varphi(z) = 0$$

$$\varphi(0) = \varphi(-H) = 0 \tag{6}$$

where $\varphi(z)$ represents the linear vertical mode function, C is the linear phase speed, $N(z)$ is the Brunt-Väisälä frequency.

The technical English of the manuscript is quite poor (there are more issues with plural vs singular and verb tense than I could count), to the point of interfering with the scientific messaging. I suppose this could be cleaned up during the peer review process, but the fact that equations are not properly type set, making the quantitative aspects very difficult to judge, suggests not enough care was placed on communication and that this goes beyond language issues. As a simple example, in equation (1) were the fraction typeset as a fraction, the symbol $\ast$ would be unnecessary and potential confusion with the use of $\ast$ to denote convolution could be avoided.

Response: Thank you for your valuable comment. We feel very sorry for our poor technical English and the equations are not properly typeset. We have tried our best to correct the issues with plural vs singular and verb tense in the revised manuscript. And we have also tried our best to properly typeset the equations in the revised manuscript. In equation (2) of the revised manuscript, we have deleted the symbol "$\ast$". The revised equation is shown as follow:

$$\lambda = \lambda_s - x_w = \lambda_s - \frac{\lambda_s}{V_{ship}}V_{water} \tag{2}.$$

The technical graphics (13 figures) are quite good, with nicely put together Matlab figures and a very nice diagram in Figure 2. Some figures could use grid lines, and Fig 9 could use a better symbol (a filled triangle, '^', or pentagram, 'p' with 'MarkerFaceColor' set in the plot command). I was really surprised that no plots of the density profile the waves propagate on were provided (even in schematic form).

Response: Thank you for your valuable suggestion and comment. We have used gridlines in Fig 9 and Fig 10 of the revised manuscript. And a better symbol (a filled triangle) has been used in Fig 9 of the revised manuscript. Previous scholars demonstrated that seismic reflections generally track isopycnal surfaces (Holbrok et al., 2013; Krahmann et al., 2009; Sheen et al., 2011). We believe the seismic stacked sections (like Fig 3 and Fig 4) include the information of the density profile. So we did not provide the plots of the density profile the waves propagate on (even in schematic form). We have added the above description in section 2 (Data and Methods) of the revised manuscript (lines 104-107).
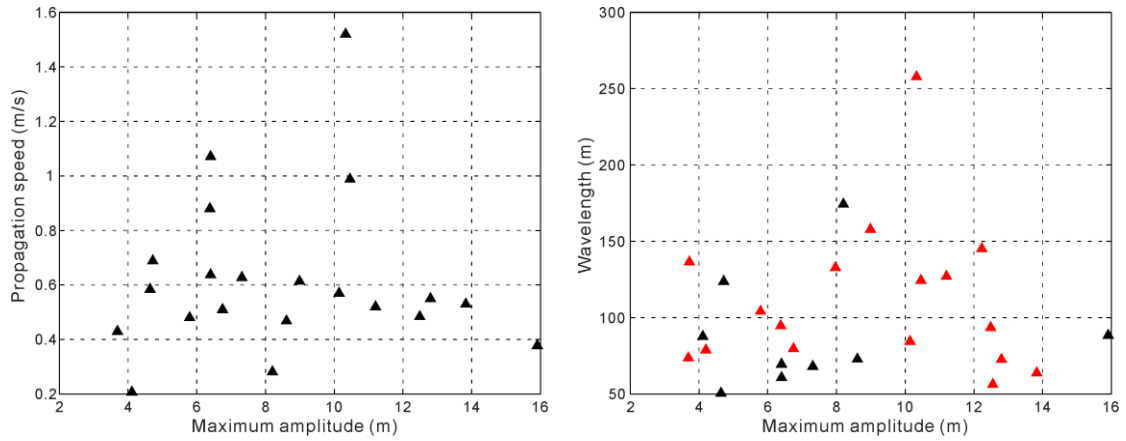
Figure 9. (a) The relationship between the propagation speeds and the maximum amplitudes of the mode-2 ISWs observed in the study area. (b) The relationship between the wavelengths and the maximum amplitudes of the mode-2 ISWs observed in the study area. The black and red crosses denote the ISWs on the survey lines in the SW-NE direction and in the NE-SW direction, respectively.
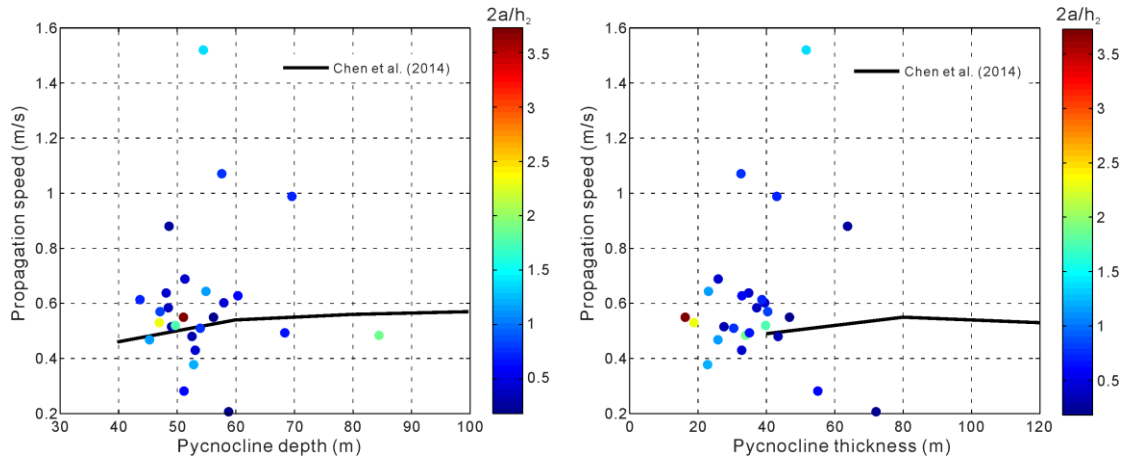
Figure 10. (a) The relationship between the propagation speeds and the pycnocline depths of the mode-2 ISWs observed in the study area. (b) The relationship between the propagation speeds and the pycnocline thicknesses of the mode-2 ISWs observed in the study area. The color filled circle indicates the dimensionless amplitude.

Many of the fits shown are very poor (Fig 7,8,10) to the point where there really isn't much one can conclude scientifically (e.g. saying that the red crosses in Figs. 7,8 follow Kozlov and Makarov, as the authors do is rather dubious). For Figure 12, what would a "good fit" be? The procedure for how the red curve in this figure is computed is not clearly described.

Response: Thank you for your valuable comment. We acknowledge that many of the fits shown are not very good. We think it is the result of the multi-parameter controlling in the actual ocean. We have changed our descriptions of the fitting results in the revised manuscript to avoid being too absolute. We could not find a "good fit" for Figure 12 based on the basic KdV theory. Maybe it needs other theory to fit this kind of vertical amplitude structure. We hope it could be solved in the following study. The above description has been added in

section 3.3 of the revised manuscript (lines 509-511). We have also added a more detailed description of how the red curves (considering first-order nonlinear correction) in Figures 11 and 12 are computed in section 3.3 of the revised manuscript (lines 470-477). We show the revised text (lines 470-477) as follow:

T(z) is the first-order nonlinear correction term. *T(z)* satisfies an inhomogeneous equation as follow (Grimshaw et al., 2002, 2004):

$$\frac{d^2T(z)}{dz^2} + \frac{N(z)^2}{C^2}T(z) = -\frac{\alpha}{C}\frac{d^2\varphi(z)}{dz^2} + \frac{3}{2}\frac{d}{dz}\left[\left(\frac{d\varphi(z)}{dz}\right)^2\right] \tag{8}$$

$$T(0) = T(-H) = 0$$

$$\alpha = \frac{3C}{2}\frac{\int_{-H}^{0}\left(\frac{d\varphi(z)}{dz}\right)^3 dz}{\int_{-H}^{0}\left(\frac{d\varphi(z)}{dz}\right)^2 dz} \tag{9}$$

where α is the quadratic nonlinear coefficient. Equation (8) has a unique solution by adding the restriction condition of *T(z$_{max}$)=0* (Grimshaw et al., 2002), where z_{max} represents the depth of the maximum amplitude of ISW. The detailed calculation process is described in Gong et al. (2021).

I don't want to pile on, and I feel the methodology is quite novel and hence deserves its place in the literature, but the theoretical errors must be fixed before this work is published. So let me lay out what I feel the bottom line is:

1. Comment: The theoretical side of this manuscript needs to be cleaned up. The term "phase velocity" needs to be removed, or the authors have to define what it means for ISWs. Equations must be properly typeset, and not just thrown into text as ratios (you could for example define commonly used ratios (e.g. $\tilde{a}=2a/h_2$ and then refer to $\tilde{a}$ in the text).

1. Reply: Thank you for your valuable comment and suggestion. We have changed all the "phase velocity" into "propagation speed" in the revised manuscript. We have also tried our best to properly typeset the equations in the revised manuscript. In equation (2) of the revised manuscript, we have deleted the symbol "*", and the revised equation (2) are shown as follow:

$$\lambda = \lambda_s - x_w = \lambda_s - \frac{\lambda_s}{V_{ship}}V_{water} \tag{2}.$$

We have defined commonly used ratios to avoid throwing them into text in the revised manuscript (we define *ã=2a/h₂*, *λ₀=2λ/h₂*, *Ũ=U_c/C*, and then refer to *ã, λ₀, Ũ* in the text).

2. Comment: Fits need to have R values computed (Matlab will do this via the "tools" button on the figure, or from the command line) and these need to be reported in tables.

2. Reply: Thank you for your valuable comment and suggestion. We have computed the R^2 values for the fits in Figures 7, 8, 10, 11, and 12. And we have respectively reported them in Tables 3, 4, 5, 6, and 7 of the revised manuscript. We have also added the related description in the text of the revised manuscript (like lines 315-318, lines 335-338, lines 477-480). We show the revised text (lines 315-318, lines 335-338, lines 477-480) as follow:

The fitting effects of Kozlov and Makarov (1990), Salloum et al. (2012), and the segmentation fitting in Fig. 7 are shown in Table 3. The segmentation fitting computed by ourselves in Fig.

7 can be expressed by the equation as follow:

$$\tilde{U} = \frac{9.441\tilde{a}^4 - 27.19\tilde{a}^3 + 28.14\tilde{a}^2 - 10.93\tilde{a} + 1.016}{\tilde{a} - 0.6401} \tag{4}$$

The fitting effects of Salloum et al. (2012) and the segmentation fitting in Fig. 8 are shown in Table 4. The segmentation fitting computed by ourselves in Fig. 8 can be expressed by the equation as follow:

$$\lambda_0 = 1.865\tilde{a} + 2.066 \tag{5}$$

The fitting effects of the linear vertical mode function and the first-order nonlinear vertical mode function in Figs. 11 are shown in Table 6. We comprehensively evaluate the goodness of fitting by the computed R2, the depths corresponding to the maximum amplitude between the observation results and the fitting results, and the overall trends between the observation results and the fitting results.

Table 3. The Fitting Effects of Each Curve in Figure 7 on the Observation Points.

$\tilde{a}$ range	fitting curve	R^2
larger than 1.18	Benjamin (1967)	0.34
smaller than 1.18	Kozlov and Makarov (1990)	0.67
smaller than 1.18	Salloum et al. (2012)	less than 0
smaller than 1.18	segmentation fitting	0.39

Note. For the fitting curve of Kozlov and Makarov (1990), we use the three red cross observation points to compute the R^2 value. For the fitting curves of Salloum et al. (2012) and segmentation fitting, we use the black cross observation points, whose $\tilde{U}$ are less than 2, to compute the R^2 values.

Table 4. The Fitting Effects of Each Curve in Figure 8 on the Observation Points.

$\tilde{a}$ range	fitting curve	R^2
larger than 1.87	Salloum et al. (2012)	less than 0
larger than 1.87	segmentation fitting	0.97
smaller than 1	Benjamin (1967)	less than 0

Table 5. The Fitting Effects of Each Curve in Figure 10 on the Observation Points.

figure	fitting curve	R^2
Figure 10a	Chen et al. (2014)	less than 0
Figure 10b	Chen et al. (2014)	less than 0

Note. For the fitting curve of Chen (2014) in Fig. 10a, we use the observation points, whose propagation speeds are less than 0.8 m/s and larger than 0.21 m/s, to compute the R^2 value. For the fitting curve of Chen (2014)

in **Fig. 10b, we use the observation points, whose propagation speeds are less than 0.9 m/s and pycnocline thicknesses are larger than 40 m, to compute the R^2 value.**

Table 6. The Fitting Effects of Each Curve in Figure 11 on the Observation Points.

ISW#	seawater depth range	fitting curve	R^2
ISW1	39-70 m	blue curve	0.98
		red curve	0.99
ISW2	39-63 m	blue curve	0.96
		red curve	0.88
ISW2	63-73 m	blue curve	less than 0
		red curve	0.09
ISW3	39-72 m	blue curve	0.59
		red curve	0.4
ISW4	42-86 m	blue curve	0.72
		red curve	0.71
ISW5	38-97 m	blue curve	0.81
		red curve	0.94
ISW6	36-82 m	blue curve	0.97
		red curve	0.94
ISW7	41-66 m	blue curve	0.8
		red curve	0.91
ISW7	66-85 m	blue curve	0.77
		red curve	less than 0
ISW8	36-85 m	blue curve	0.95
		red curve	0.95
ISW9	41-74 m	blue curve	1
		red curve	0.8
ISW10	36-42 m	blue curve	less than 0
		red curve	less than 0
ISW10	42- 73 m	blue curve	0.99
		red curve	0.65

Table 7. The Fitting Effects of Each Curve in Figure 12 on the Observation Points.

ISW#	seawater depth range	fitting curve	R^2
ISW11	37-101 m	blue curve	0.22
		red curve	0.3
ISW12	30-75 m	blue curve	0.47
		red curve	0.68
ISW16	29-78 m	blue curve	0.46
		red curve	0.25
ISW17	29-79 m	blue curve	less than 0
		red curve	less than 0

3. Comment: Give some idea as to the vertical structure of the density field. The readers should understand why the authors want to provide the fits that they do, and they need to have a context for how the density may be changing due to various environmental factors.

3. Reply: Thank you for your valuable comment. We have added these contents in the corresponding place in section 3.3 of the revised manuscript (lines 390-415). We also show the revised text (lines 390-415) as follow:

The vertical distribution of ISW amplitude (the vertical displacement of isopycnal) is called its vertical structure. ISWs have different modes, which correspond to different vertical structures (Fliegel and Hunkins, 1975). Previous scholars have used different theoretical models to study the vertical structure of ISW amplitude (Fliegel and Hunkins, 1975; Vlasenko et al., 2000; Small and Hornby, 2005). Among them, only Vlasenko et al. (2000) compared the results of numerical simulation with the results of local observations. And they found that the depths correspond to the ISW maximum amplitude (the maximum vertical displacement of isopycnals) given by the two are in good agreement with each other. At present, there is less work comparing the theoretical vertical structure of mode-2 ISW amplitude with the observed results. This work is conducive to improving our understanding of the vertical structure of the mode-2 ISW in the ocean (including the factors that affect the vertical structure). It can also test the validity and applicability of the theoretical vertical structure to a certain extent. The seismic oceanographic method has a high spatial resolution, and its clear imaging results of ISWs are more conducive to the study of vertical structure. The vertical structure of ISW amplitude is controlled by a variety of environmental factors. Geng et al. (2019) used the seismic oceanography method to study the vertical structure of ISW amplitude near Dongsha Atoll in the South China Sea. It is found that when the ISW interacts intensely with the seafloor, the observed vertical structure of ISW amplitude may be significantly different from the theoretical result. Gong et al. (2021) compared the vertical structure of ISW estimated by theoretical models with the vertical structure of ISW observed by the seismic oceanography method. And they analyzed in detail the factors affecting the vertical structure of ISW amplitude near Dongsha Atoll in the South China Sea. It is found that the vertical structure of ISW is mainly controlled by nonlinearity. It usually appears that the quadratic nonlinear coefficients of ISWs that conform to the linear vertical structure function are small, while the quadratic nonlinear coefficients of ISWs conforming to the first-order nonlinear vertical structure function are larger. In addition, topography, ISW amplitude, seawater depth, and background flow may all affect the vertical structure of ISW amplitude. It appears that larger seawater depth may weaken the influence of the nonlinearity of the ISW on the vertical structure, making the vertical structure of ISW more in line with linear theory. Larger amplitude will make ISW more susceptible to the influence of topography, which will change the vertical structure. Vlasenko et al. (2000) observed that the vertical structure of ISW has local extrema. They thought it is caused by smaller-scale internal waves. In addition, the background flow shear also has an important effect on the vertical structure (Stastna et al., 2002; Liao et al., 2014). Xu et al. (2020) found that the background flow at the center of the eddy can weaken the amplitude of ISW.

4. Comment: I would strongly suggest having a look at the various JPO papers on the Pt Sal

internal wave "mega project"; the two McSweeney et al papers especially. Some of these papers included using KdV theory to examine environmental variability in a way that may be useful to the authors, others adopted different points of view which the authors may find useful to put their results in context.

4. Reply: Thank you for your valuable suggestion. We have added these contents in Table 1 and the corresponding place in section 4 of the revised manuscript (lines 572-600). We also show the revised text (lines 572-600) as follow:

McSweeney et al. (2020a, 2020b) conducted observational studies on the cross-shore and alongshore evolution characteristics of internal bores near Point Sal, California. They used the quadratic nonlinear coefficient α calculated by KdV theory to characterize the stratification. And they found that when the α calculated from the background density is greater than 0, the waveform of the internal bore becomes steep as the internal bore passes the site. When the α calculated from the background density is less than 0, the waveform of the internal bore becomes rarefied as the internal bore passes the site. Background stratification affects the evolution of internal bores. And the passage of an internal bore will also change the stratification, which in turn affects the evolution of a subsequent internal bore. They found that the change in the α after the internal bore passed is positively correlated with the background α. By analogy with the work of McSweeney et al. (2020a, 2020b), we calculated the background quadratic nonlinear coefficient α (corresponding to the stratification before the arrival of the ISW) and the linear phase speed C, at the position of the ISWs in the study area by solving Eq. (6) and Eq. (9). Because the theoretical vertical structures calculated based on the KdV theory cannot well fit the observed vertical structures of the ISWs on the survey line L74 (Fig. 12). We are not sure that the KdV theory can well describe the ISWs appearing on the survey line L74. Therefore, we have only calculated the α and C at each ISW position on the survey line L84. The calculation results show in columns 12 and 13 of Table 1, respectively. Observing the calculated α values in Table 1, we find that the α values of ISW1-ISW4 are all less than 0. And the α values of ISW5-ISW10 are all greater than 0. It corresponds well to the waveform characteristics of the ISWs in Fig. 3. That is, for ISW1-ISW4 whose α values are less than 0, their waveforms are relatively rarefied. For ISW5-ISW10 whose α values are greater than 0, their waveforms are relatively steep. It indicates that the background stratification has an influence on the shape of the mode-2 ISWs in the study area. Observing the calculated C values in Table 1, we find that from ISW1 to ISW4, the calculated C values gradually decrease with the decreasing seafloor depths. It is consistent with the observed trend that the propagation speeds U_c of the ISWs (column 11 of Table 1) also gradually decrease with the decreasing seafloor depths. ISW5 is shallower than ISW4. But the calculated C and the observed U_c of ISW5 are both greater than those of ISW4. From ISW5 to ISW10, as the seafloor depths gradually decrease, the calculated C values and the observed ISW U_c values overall show a decreasing trend again. We think the above phenomenon is caused by background stratification. That is, ISW1-ISW4 have a similar background stratification. And ISW5-ISW10 have another similar background stratification. It makes the calculated C values and observed U_c values of SW1-ISW4 decrease with the decreasing of seafloor depths. The calculated C and observed U_c of ISW5 are greater than those of ISW4. On the whole, the calculated C values and the observed U_c values of ISW5-ISW10 decrease with the decreasing of seafloor depths. The above discussion indicates that the background stratification has an

influence on the propagation speeds of the mode-2 ISWs in the study area.

Table 1. Characteristic Parameters of the 10 Mode-2 Internal Solitary Waves in Survey Line L84.

ISW#	H (m)	A (m)	a (m)	h_2 (m)	$2a/h_2$	...	$2\lambda/h_2$	U_c (m/s)	α (s^{-1})	C (m/s)
ISW1	145.5	3	2.22	29.23	0.15	...	7.09	0.85±0.6	-0.018	0.384
ISW2	138.8	4.7	5.84	25.93	0.45	...	9.55	0.69±0.19	-0.0179	0.382
ISW3	130.5	4.1	4.45	27.6	0.32	...	6.13	0.52±0.12	-0.0181	0.378
ISW4	121.5	5.2	6.04	34.72	0.35	...	3.18	0.19±0.11	-0.018	0.372
ISW5	111	6.79	12.67	40.84	0.62	...	4.67	0.32±0.16	0.0068	0.391
ISW6	108	4.6	7.5	37.19	0.4	...	2.72	0.58±0.16	0.0108	0.389
ISW7	104.3	6.4	7.34	34.83	0.42	...	3.49	0.64±0.28	0.0158	0.386
ISW8	103.5	13.2	15.82	32.94	0.96	...	4.43	0.46±0.24	0.0155	0.385
ISW9	103.5	15.9	13.56	22.79	1.19	...	7.76	0.38±0.17	0.0161	0.385
ISW10	102.8	13.6	15.87	20.62	1.54	...	9.13	0.55±0.34	0.0164	0.384

Note. H, seafloor depths. A, maximum amplitudes. a, equivalent ISW amplitudes. h_2, equivalent pycnocline thicknesses. λ, equivalent wavelengths. U_c, apparent propagation speeds obtained from seismic observation. α, quadratic nonlinear coefficient shown in Ea. (9) and is obtained by solving Eq. (6). C, linear phase speed which is obtained by solving Eq. (6).

McSweeney, J. M., Lerczak, J. A., Barth, J. A., Becherer, J., Colosi, J. A., MacKinnon, J. A., MacMahan, J. H., Moum, J. N., Pierce, S. D., and Waterhouse, A. F.: Observations of shoaling nonlinear internal bores across the central California inner shelf, Journal of Physical Oceanography, 50, 111-132, https://doi.org/10.1175/JPO-D-19-0125.1, 2020a.

McSweeney, J. M., Lerczak, J. A., Barth, J. A., Becherer, J., MacKinnon, J. A., Waterhouse, A. F., Colosi, J. A., MacMahan, J. H., Feddersen, F., Calantoni, J., Simpson, A., Celona, S., Haller, M. C., and Terrill, E.: Alongshore variability of shoaling internal bores on the inner shelf, Journal of Physical Oceanography, 50, 2965-2981, https://doi.org/10.1175/JPO-D-20-0090.1, 2020b.

5. Comment: Ask a colleague to read strictly for language. Even those like myself, for whom English isn't their first language, could catch simple mistakes (e.g. tense).
5. Reply: Thank you for your valuable suggestion. We have asked a colleague to read strictly for language and corrected the grammar mistakes of the manuscript.